frontiers | Frontiers in Pharmacology

TYPE Methods
PUBLISHED 24 November 2022
DOI 10.3389/fphar.2022.1040039

OPEN ACCESS

EDITED BY
Choel Kim,
Baylor College of Medicine,
United States

REVIEWED BY
Benedict-Tilman Berger,
Goethe University Frankfurt, Germany
Matthew Robert Groves,
University of Groningen, Netherlands
Lei Sun,
Henan University, China
Pierfausto Seneci,
University of Milan, Italy

*CORRESPONDENCE
Bolormaa Baljinnyam,
bolormaa.baljinnyam@nih.gov
Anton Simeonov,
anton.simeonov@nih.gov

SPECIALTY SECTION
This article was submitted to Experimental Pharmacology and Drug Discovery, a section of the journal Frontiers in Pharmacology

RECEIVED 08 September 2022
ACCEPTED 04 November 2022
PUBLISHED 24 November 2022

CITATION
Ronzetti MH, Baljinnyam B, Itkin Z, Jain S, Rai G, Zakharov AV, Pal U and Simeonov A (2022), Application of temperature-responsive HIS-tag fluorophores to differential scanning fluorimetry screening of small molecule libraries.
Front. Pharmacol. 13:1040039.
doi: 10.3389/fphar.2022.1040039

Application of temperature-responsive HIS-tag fluorophores to differential scanning fluorimetry screening of small molecule libraries

Michael H. Ronzetti[1,2], Bolormaa Baljinnyam[1]*, Zina Itkin[1], Sankalp Jain[1], Ganesha Rai[1], Alexey V. Zakharov[1], Utpal Pal[2] and Anton Simeonov[1]*

[1]National Center for Advancing Translational Sciences, National Institutes of Health, Rockville, MD, United States, [2]Department of Veterinary Medicine, College of Agriculture and Natural Resources, University of Maryland, College Park, MD, United States

Differential scanning fluorimetry is a rapid and economical biophysical technique used to monitor perturbations to protein structure during a thermal gradient, most often by detecting protein unfolding events through an environment-sensitive fluorophore. By employing an NTA-complexed fluorophore that is sensitive to nearby structural changes in histidine-tagged protein, a robust and sensitive differential scanning fluorimetry (DSF) assay is established with the specificity of an affinity tag-based system. We developed, optimized, and miniaturized this HIS-tag DSF assay (HIS-DSF) into a 1536-well high-throughput biophysical platform using the Borrelial high temperature requirement A protease (BbHtrA) as a proof of concept for the workflow. A production run of the BbHtrA HIS-DSF assay showed a tight negative control group distribution of T_m values with an average coefficient of variation of 0.51% and median coefficient of variation of compound T_m of 0.26%. The HIS-DSF platform will provide an additional assay platform for future drug discovery campaigns with applications in buffer screening and optimization, target engagement screening, and other biophysical assay efforts.

KEYWORDS

high-throughput sceening, differential scanning fluorimetry, biophysical screening, small molecule screening, biochemistry

Introduction

Modern drug discovery programs and their myriad of targets demand a toolbox with multiple assay types for the rapid high-throughput screening and confirmation of small molecule libraries to identify new therapeutic ligands. The main purpose of early-stage assays is to provide hits in an expedient and decisive path towards lead optimization. An indispensable biophysical technique for these types of screens is the thermal shift assay,

also known as differential scanning fluorimetry (DSF), as it presents both a material- and cost-efficient manner of profiling engagement to a target without the need for a functional assay (Pantoliano et al., 2001). By utilizing a dye like SYPRO Orange that alters its fluorescence upon binding to hydrophobic patches in proteins, the unfolding dynamics of a target can be followed through a temperature gradient (Niesen et al., 2007).

Changes in the observed unfolding behavior of a target protein can be caused by ligands binding to the protein and imparting free-energy contributions that shift the Gibb's free energy of unfolding, often seen as a stabilization of the protein in response to the temperature gradient (Baljinnyam et al., 2020b; Gao et al., 2020). The ease of use and ability of the DSF assay to detect binding over a wide-range of affinities have led to its continued deployment in drug discovery affinity screens for small molecule binders and fragment screens towards a target protein (Amaning et al., 2013; Simeonov, 2013; DeSantis and Reinking, 2016; Christine and Wright, 2017; Gao et al., 2020; Krasavin et al., 2020; Li and Zhang, 2021). Beyond screening, there is a significant diversity of manners in which the DSF assay is applied, including buffer and crystallization formulation and binding mechanism studies. Extending these applications, DSF was recently applied to improving refolding conditions of protein after denaturing purifications (Biter et al., 2016; Wang et al., 2017; Lee et al., 2019; Ronzetti et al., 2022). The thermal shift technique has also been applied to more complex protein-protein interactions and for the quantification of overexpressed protein in lysates (Seo et al., 2014; Shao et al., 2020).

While the robustness of the DSF assay gives it a broad applicability in both sample preparation and small molecule screening, there are limitations to the assay in the standard form that relies on extrinsic dye (Simeonov, 2013; Nie et al., 2022). The environment-sensing dyes present a non-specific signal that is prone to interference from commonly employed buffer components and detergents (Simeonov, 2013; Gao et al., 2020). Additionally, the assay is optimally set up in systems with a single protein species present, whereas the presence of additional cofactors or binding partners will give rise to complex and difficult to interpret signal. These limitations could be improved on by employing a fluorophore with a red-shifted emission wavelength that is relatively agnostic to buffer conditions.

The Borrelial high temperature requirement A (BbHtrA) protein is a member of the HtrA family, a group of proteases widely expressed across the animal kingdom and essential to the survival and infectivity of a number of microbes of concern to public health (Pallen and Wren, 1997; Clausen et al., 2002; Krojer et al., 2002; Ibrahim et al., 2004; Zurawa-Janicka et al., 2010; Clausen et al., 2011; Backert et al., 2018; Cho et al., 2020). BbHtrA is a therapeutic target of interest in *Borrelia burgdorferi* due to its involvement in borrelial invasion and dissemination in the human host and may play a role in late-stage symptoms of Lyme disease (Gherardini, 2013; Kariu et al., 2013; Russell et al., 2013; Stricker and Johnson, 2013; Kariu et al., 2015; Ye et al., 2016; Zhuang et al., 2018; Bernard et al., 2019; Thakur et al., 2022). In this manuscript, we describe the application of a fluorophore, linked to the protein of interest *via* an affinity tag, that results in a more agnostic, specific signal in a DSF setting, as well as the optimization and production of 384- and 1536-well assays to screen for small molecule binders to HIS-tagged BbHtrA.

Materials and methods

Protein and reagents

Borrelia burgdorferi HtrA wildtype (WT) and catalytically-inactive S226A mutant (S/A) were expressed and purified as previously described (Ronzetti et al., 2022). The HIS-tag fluorophores RED-tris-NTA 2nd Gen (NanoTemper, #MO-L018) and Atto-647 (Sigma, #02175), were both suspended in PBS at 5 μM, aliquoted, and stored at −20°C.

Casein-BODIPY cleavage assay

Protease activity was profiled using a casein substrate that has been labeled with a molar excess of BODIPY TR-X dye (ThermoFisher, EnzChek Protease Activity Kit). To construct the assay plate, 200 nL of compounds (1% DMSO v/v final DMSO 1%) and DMSO (negative control) were dry spotted into 384-well black plates (Greiner, #782096) and immediately mixed with 16 μl of 62.5 nM BbHtrA WT (50 nM final concentration), spun down, and incubated for 15 min at room temperature. Then, 4 μl of 25 μg/mL casein-BODIPY (5 μg/mL final concentration) was added to each well, mixed, spun down, and immediately read on a Tecan Infinite M1000 in kinetic mode for 20 min with the following instrument settings: excitation wavelength = 590 nm ± 10; emission wavelength = 645 ± 20; gain = 95. An increase in fluorescence indicates the proteolytic liberation of fluorescent peptide fragments from the casein-BODIPY substrate, enabling comparison of proteolytic digestion rates between the DMSO, compound, and no-enzyme controls. Dose-response curves were fit using a four-parameter log logistic fit for the replicate reactions.

Casein digestion using SDS-PAGE

Proteolytic activity was profiled against native casein protein by SDS-PAGE to detect proteolytic fragments after incubation with BbHtrA. Briefly, 500 nM BbHtrA WT was mixed with 100 μM of small molecule (1% DMSO v/v final DMSO 1%) for 15 min at room temperature. Then, casein was added to a final concentration of 25 μM and incubated for 90 min at room temperature. After the

reaction, 15 µl of each sample was mixed with 4X LDS sample buffer (ThermoFisher, #NP0007) with reducing agent (ThermoFisher, #NP0009) and separated on a 10% bis-tris gel (ThermoFisher, #NP0315) with MES running buffer. The gel was then washed 4 times for 5 min each with deionized water and stained with Imperial Blue stain (ThermoFisher, #24615) for 2 hours before washing in deionized water overnight. The stained gel was then imaged using a ChemiDoc MP with default Coomassie Blue imaging settings.

Microscale thermophoresis

The binding affinity of RED-tris-NTA and Atto-647-NTA against HIS-tagged BbHtrA was evaluated by microscale thermophoresis, a technique that uses localized temperature gradients to perform biophysical interaction studies (Jerabek-Willemsen et al., 2011). First, a 16-point 1:1 serial dilution of 4 µM BbHtrA S/A (2 µM–0.06 nM final concentration) was made in PBS-T (pH 7.4, 0.01% Tween-20) in a final volume of 10 µl. Then, 10 µl of a 10 nM solution (5 nM final) of either fluorophore in PBS-T was added to each point of the BbHtrA S/A titration, mixed, and incubated in the dark at room temperature for 30 min. Samples were then loaded into standard capillaries and read on a NT.Automated (Nanotemper) using 10% excitation energy and "medium" MST power settings. All MST data was analyzed using MO.AffinityAnalysis software (Nanotemper) and fit using the time period +0.5 to +1.5 s after application of the IR laser. Data was checked for sharp capillary shapes with a single peak and consistent initial fluorescence before application of the IR laser. Normalized fluorescence values were then fit using the standard K_d model derived from the law of mass action with the concentration of fluorophore fixed at 5 nM.

HIS-tagged differential scanning fluorimetry

The Roche LightCycler 480 II and Roche LightCycler 1536 were used to run HIS-DSF assays with the 618 nm and 660 nm filters used for excitation and emission, respectively. The optimal labeling reaction was determined by creating a matrix of 7 µM 1:1 BbHtrA S/A and 500 nM 1:2 Red-tris-NTA dispensed in equal volumes onto Roche 384 well PCR plates by ECHO 550 acoustic liquid handling, incubated for 30 min at room temperature, and then sealed with optically transparent seals (Roche #04729757001) before loading into the Roche 480 II qPCR instrument. Samples were melted in standard thermal unfolding mode with a thermal gradient from 20 to 95°C at maximum ramping speed with 4 acquisitions per degree. The raw thermal curves were then analyzed to derive T_m values by the maximum first derivative method using Roche Thermal Shift analysis software.

Once optimized, a fresh mixture of the optimal BbHtrA S/A HIS-DSF labeling reaction was made for each experiment. Briefly, 3 µM HIS-tagged BbHtrA S/A was mixed with 200 nM Red-tris-NTA dye in PBS (1X, pH 7.4) and incubated for 30 min at room temperature. 10 nL of 10 mM small molecules (final concentration 100 µM) or DMSO (negative vehicle control) were dispensed using the ECHO 550 into Roche PCR assay plates (384 or 1536-well) and spun down at 1,250 x g prior to dispensing labeled protein into the assay plate. The assay plates were sealed with clear optical foil, centrifuged again, and run immediately on a Roche 480 II or Roche 1536 qPCR instrument. Standard melting curve settings were used with a thermal gradient from 37 (instrument minimum temperature) to 95°C at maximum ramping speed with 4 acquisitions per degree. Data was exported from the qPCR software and analyzed using the Roche Thermal Shift analysis software. The Roche T_m-calling analysis correlates the peak of -(d/dT) fluorescence to call the midpoint of protein melting, or T_m.

Nano-differential scanning fluorimetry and backscattering assays

Real-time monitoring of fluorescence emission at 330 nm and 350 nm (excitation wavelength: 280 nm) and backscattering absorbance of BbHtrA S/A samples in the presence of compound was performed using a NanoTemper Prometheus NT.48 instrument. First, 10 µM BbHtrA S/A was incubated with 100 µM compound or DMSO for 15 min at room temperature. Then, samples were loaded into standard capillaries, loaded onto the capillary tray, and the temperature was increased from 25 to 95°C with a ramp rate of 2.0°C/min. Since the small molecules that were tested interfered with the signal in the UV range of the instrument, the backscattering absorbance was used and plotted as a function of temperature. Three biological replicates were carried out for each condition, and their means and standard deviations are depicted.

Data analysis

All data, figures, and statistical analyses were generated using GraphPad Prism 9.

Results

Establishing the HIS-tag differential scanning fluorimetry assay

To provide target engagement data in a target-agnostic manner for our screening campaign, we sought to develop a biophysical thermal-shift based method that was amenable to

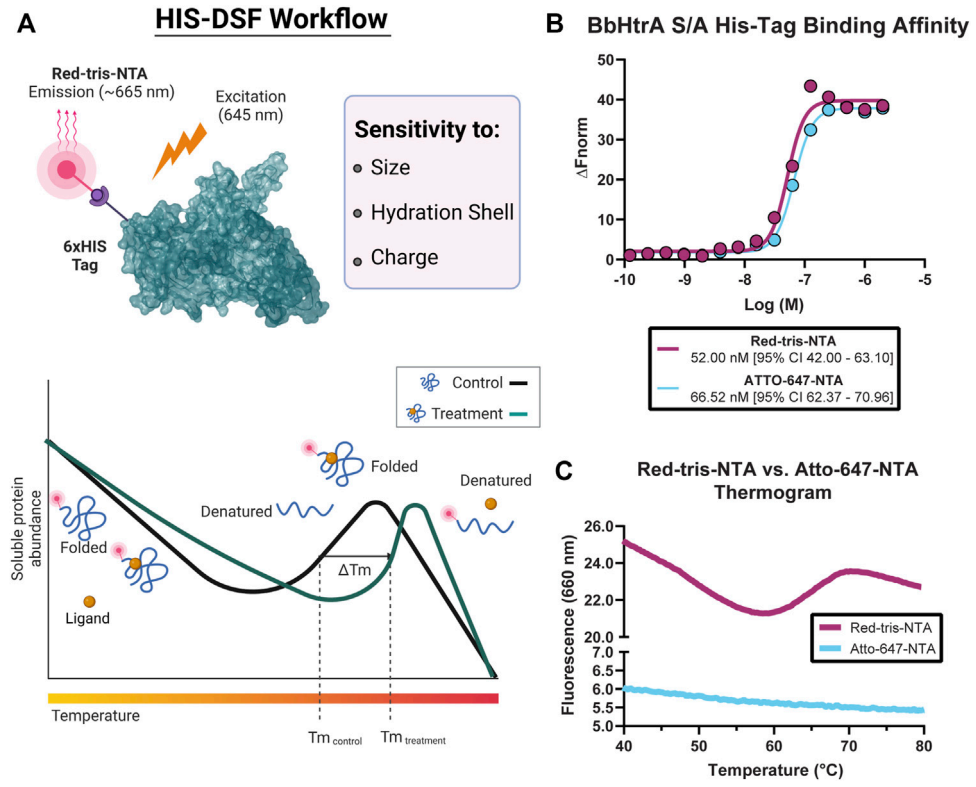

FIGURE 1
Overview of the histidine-tagged differential scanning fluorimetry assay (HIS-DSF). **(A)** Schematic representation of the His-tagged protein of interest labeled specifically by the Red-tris-NTA fluorophore by the Ni(II)-nitrilotriacetic acid (NTA) moiety (top) and the design and workflow of the HIS-DSF assay (bottom). **(B)** Evaluation of the affinity for the NTA-fluorophores towards HIS-tagged BbHtrA S/A by MST. **(C)** Testing HIS-tag directed fluorophores in a differential scanning fluorimetry experiment. Labeled protein (as described in the *Materials and Methods* section) was run in a standard DSF melting experiment to check for the presence of melting curves.

1536-well high-throughput format. The assay was also intended to be adaptable to other targets and more tolerant of buffer conditions that interfere with traditional, SYPRO Orange-based thermal shift experiments. Conceivably, a fluorophore that is directly linked to the protein of interest and gives different quantum yields dependent on the surrounding protein structure could enable this endeavor (Figure 1A).

Testing HIS-tag fluorophore properties and binding to BbHtrA

Toward these goals, we sought to profile two commercial dyes, Red-tris-NTA and ATTO-647-NTA, for their performance in differential scanning fluorimetry experiments. First, both fluorophores emit at ~650–660 nm, which reduces interference with the intrinsic fluorescence of the library compounds for screening. Second, the dyes possess a Ni(II)-nitrilotriacetic acid (NTA) moiety, which enables specific labeling of HIS-tagged proteins (Figure 1A).

The affinity of the fluorophores towards the HIS-tagged BbHtrA protein was tested using microscale thermophoresis. Both NTA fluorophores have a similar binding affinity for BbHtrA S/A, with Red-tris-NTA and ATTO-647-NTA binding to the target protein with K_d of 52.00 and 66.52 nM, respectively (Figure 1B). Interestingly, while Atto-647 and Red-tris-NTA demonstrate similar affinities for HIS-tagged BbHtrA S/A, only the Red-tris-NTA fluorophore can produce the typical DSF melting curve when tested in a thermal ramp (Figure 1C).

Miniaturization and optimization of the differential scanning fluorimetry assay

The ideal combination of probe and target protein for a DSF assay will give high signal-to-noise ratios and a tight distribution of melting temperatures in the negative control condition. To that end, the HIS-tag DSF assay was established by testing a matrix of protein and dye concentrations in 384-well format for the combination with the sharpest first derivative peak and

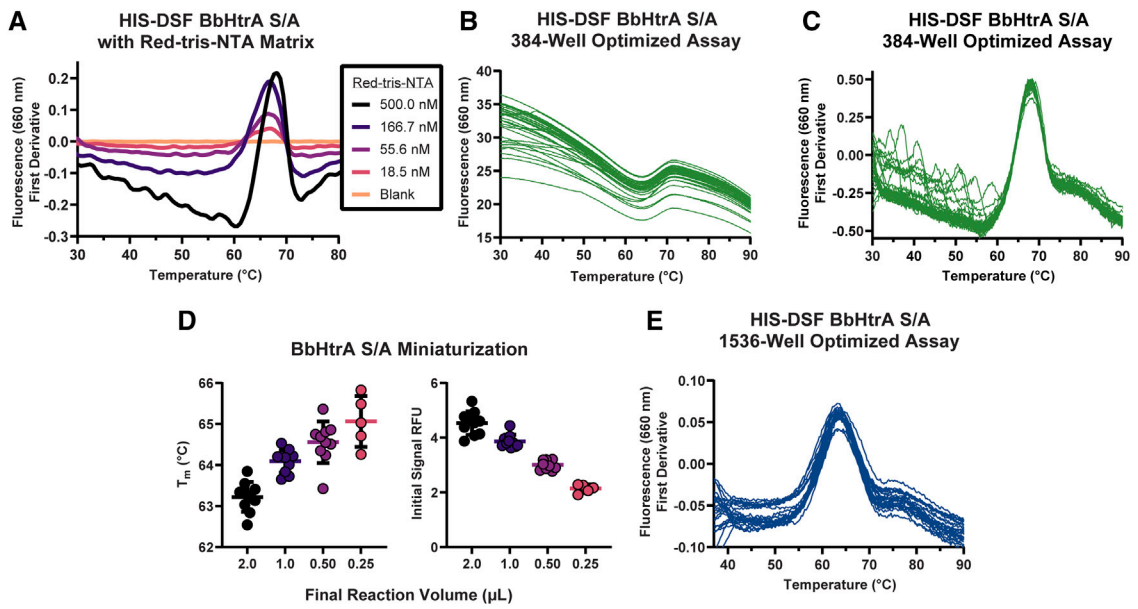

FIGURE 2
Establishing conditions and miniaturization of the HIS-DSF assay. **(A)** A titration matrix of BbHtrA S/A and Red-tris-NTA concentrations was profiled for its performance in a DSF temperature ramp. Pictured is a representative experiment of the 3.5 µM protein concentration group, with individual curves representing different concentrations of Red-tris-NTA or buffer. **(B)** Raw thermogram traces for *n* = 36 replicates of the matrix-derived best concentrations of protein and dye in 384-well format. **(C)** First derivative of the *n* = 36 replicate wells of the optimized HIS-DSF reaction. **(D)** Scatter plot of T_m and initial signal RFU values from miniaturization of the HIS-DSF BbHtrA S/A reaction into 1536-well format. Lines represent the mean of ten replicates with error bars representing the standard deviation. **(E)** The first derivatives of raw thermogram traces for *n* = 36 replicates of the optimized and miniaturized HIS-DSF BbHtrA S/A reaction in 1536-well format.

cleanest thermogram. After testing triplicate 5 µl reactions of each matrix point of BbHtrA and RED-tris-NTA, the two best conditions identified were 3 µM BbHtrA and either 500 or 166.7 nM RED-tris-NTA (Figure 2A). To minimize use of reagents, 200 nM RED-tris-NTA was chosen to move forward in continued optimization. Follow-up testing of 36 replicates of the optimized RED-tris-NTA and BbHtrA S/A reaction gave raw thermal melting curves with similar sigmoidal profiles and initial signal whose reproducibility is further exemplified in the first derivative plot of these raw melting curves (Figures 2B,C). Additionally, the peaks of the first derivative of the melting curve, defined as the T_m, are tightly grouped at 67.98°C (95% CI 67.96–68.01°C). The signal to noise ratio (S/N) for the HIS-DSF assay in 384-well format, defined as the ratio of the mean signal to the standard deviation of that signal, was calculated to be 730.8, with a percent coefficient of variation (% CV) of 0.09%.

We attempted to further miniaturize the assay to 1536-well format after modifying the excitation and emission filters in the Roche LightCycler 1536 for an appropriate set (excitation: 618 nm, emission: 640 nm). Miniaturization of the optimized BbHtrA HIS-DSF labeling mixture revealed that variation in T_m and initial relative fluorescence (RFU) signal was acceptable down to 1,000 nL total reaction volume (Figure 2D). Final testing of 36 replicates of the optimized BbHtrA HIS-DSF reaction showed an average T_m of 63.77°C (95% CI 63.66–63.97°C) with a S/N of 191.4 and negative control % CV of 0.52% (Figure 2E). It is best practice to measure the affinity of binders at low as possible concentration of the target protein (Jarmoskaite et al., 2020). The final concentration of BbHtrA in this assay was, however, dictated by the filter set of the Roche Lightcycler instruments.

Often, high-throughput screening workflows require the use of detergents in assay buffers to prevent material adsorption inside liquid handling equipment. Additionally, entire protein target classes like GPCRs and integral membrane proteins require the use of surfactants to solubilize and maintain a native protein structure. These additives are known to interfere with existing extrinsic dyes like SYPRO Orange (Simeonov, 2013). Therefore, a side-by-side comparison of BbHtrA-DSF using SYPRO Orange and Red-tris-NTA in presence of a detergent was performed. When BbHtrA S/A was incubated in the presence of increasing amounts of Tween-20 detergent (both above and below the critical micelle concentration (CMC) of~0.06% in PBS), the initial fluorescent signal of SYPRO Orange increased with higher levels of detergent that masked the thermal unfolding transition (Figure 3A). In contrast to SYPRO Orange, there are no significant perturbations to the thermogram of BbHtrA in the presence of the same

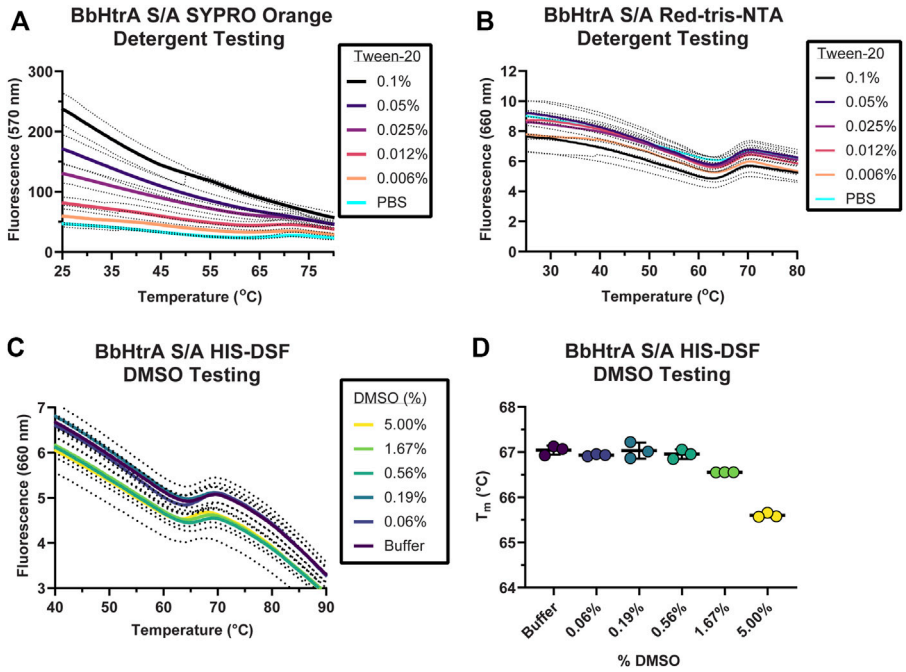

FIGURE 3
Testing buffer conditions for the HIS-DSF assay. **(A,B)** Melting behavior of BbHtrA S/A in presence of different concentrations of Tween-20 detergent reported by SYPRO Orange **(A)** or when labeled with Red-tris-NTA **(B)**. Lines represent the mean of three replicates with dots representing the standard deviation. **(C)** Raw thermogram of the optimized HIS-DSF BbHtrA S/A reaction in the presence of different concentrations of DMSO. Lines represent the mean of three replicates with dotted lines representing the standard deviation. **(D)** Scatter plot of the T_m values from the optimized HIS-DSF BbHtrA S/A reaction in the presence of different concentrations of DMSO. Lines represent the mean of three replicates with error bars representing the standard deviation.

concentrations of Tween-20 when labeled with Red-tris-NTA (Figure 3B).

The effect of DMSO was profiled on the melting behavior of BbHtrA S/A with a 5% v/v 1:2 DMSO titration, simulating the solvent concentrations that would take place in a small molecule screening campaign. The thermal unfolding profile of BbHtrA S/A did not vary significantly in any of the DMSO concentrations tested, although a slight destabilization is detected from 1.67% DMSO and above (Figures 3C,D). The stability of BbHtrA in response to DMSO was further tested using an orthogonal thermal shift-based method called nanoDSF, a differential scanning fluorimetry method that monitors shifts in tryptophan autofluorescence and backscattering aggregation signals during a thermal ramp (Krakowiak et al., 2019; Magnusson et al., 2019). In agreement with the HIS-DSF data, the onset of turbidity, or T_{onset}, did not change significantly between DMSO groups (Supplemental Figure 1A), nor did the shape of the 350 nm/330 nm ratiometric thermogram (Supplementary Figure 1B).

The specificity of Red-tris-NTA for the HIS-tagged protein was tested by labeling the protein in the presence of 50 mM EDTA and 250 mM imidazole, inhibitors of the Ni(II) ion and polyhistidine interaction. Notably, samples of BbHtrA S/A that were labeled in the presence of HIS-tag inhibitors did not produce a melting thermogram, indicating that the dye must be bound to the HIS-tagged protein to generate a melting curve (Supplementary Figure 1C).

Proof-of-concept screening of compound libraries and confirmation of hit molecules

Primary screening of a protease-targeted small molecule library

The production-readiness of the assay was tested by performing a single-dose screen in triplicate of the NCATS Protease Inhibitor library, a curated collection of 872 small molecules with known modulatory effects against a range of therapeutically-relevant proteases. To increase the robustness of our analysis on assay variation, each replicate was performed on separate days with fresh labeling reactions of BbHtrA S/A. As there are no known ligands that thermally stabilize HtrA proteins without interfering with the HIS-tag labeling ($ZnCl_2$ stabilizes HtrA proteins, inhibits the protease activity, and interferes with NTA labeling), only the negative control variation was used in

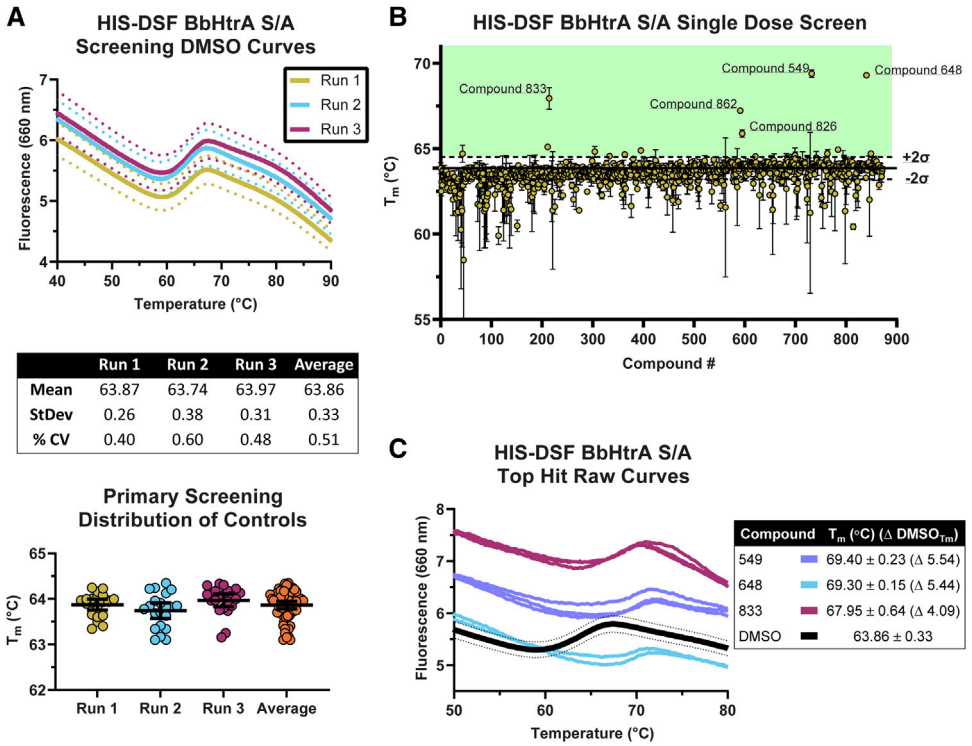

FIGURE 4
Screening of the NCATS Protease Inhibitor small molecule library using the optimized HIS-DSF assay. **(A)** Thermograms of the negative control DMSO wells from the three screening replicates. Each differently colored line represents the means of 24 negative control wells in a single replicate screening run with dotted lines representing the 95% confidence interval. Negative control wells are also clustered according to their T_m for each screening run, with whisker plots representing the mean with error bars showing the 95% confidence interval. **(B)** Distribution of the T_m values for each compound in the small molecule library arranged by masked compound ID. Each point represents the mean of the three screening runs with error bars representing the 95% confidence interval. The solid line represents the mean of the negative control DMSO wells, with dashed lines above and below representing two times the standard deviation of the negative control DMSO wells, with the green shaded area representing the area where compounds are selected for follow-up testing. **(C)** Thermograms of the top three hits in the HIS-DSF primary screen. Each line represents an individual replicate from each screening run, while the DMSO thermogram line represents the mean of the negative control wells with dotted lines representing the 95% confidence interval.

selecting compounds moving forward (Russell et al., 2016; Bernegger et al., 2020). The distribution of T_m values for the aggregated DMSO negative control group (final DMSO 1%) was in line with previous values obtained during optimization, giving an average T_m of 63.86°C ± 0.33 and an average % CV of 0.51%. The raw thermograms of the DMSO control group between runs also demonstrated low inter-run variability between traces (Figure 4A).

The cutoff for hits was made by selecting compounds that have T_m values greater than two times the standard deviation of the DMSO negative control groups. Compounds that show up as destabilizers below the DMSO control range were excluded from further analysis. Using the triplicate run average T_m of 63.86°C ± 0.33, compounds with an average T_m at or above 64.52°C were flagged as potential hits. Applying this cutoff to the primary HIS-DSF screen filtered the 872-compound library down to 16 hits, representing a primary screen hit rate of 1.83% (Figure 4B). The thermal unfolding curves for three of these hits (**549**, **648**, and **833**) reveal a consistent right-shift in the sigmoidal unfolding curves and T_m of BbHtrA S/A, indicating small molecule ligand-induced stabilization of the target (Figure 4C). The average T_m for these compounds ranged from 64.54 to 69.40°C with a median standard deviation of 0.13°C and a % CV of 0.20%. Variation was similar when analyzing the entire single-dose library screen which had a median standard deviation of 0.17°C and 0.26% CV.

Validation and counter-screening of primary screen hits

Compounds that met the cutoff from the primary screen were replated from powder stocks and tested in a 7-point 1:4 dose response curve (200 μM–12.8 nM final concentrations) with the same HIS-DSF assay using 5 biological replicates. The T_m and variation in the DMSO negative control samples was in line with previous runs (average T_m: 63.71°C, standard deviation: 0.28°C,

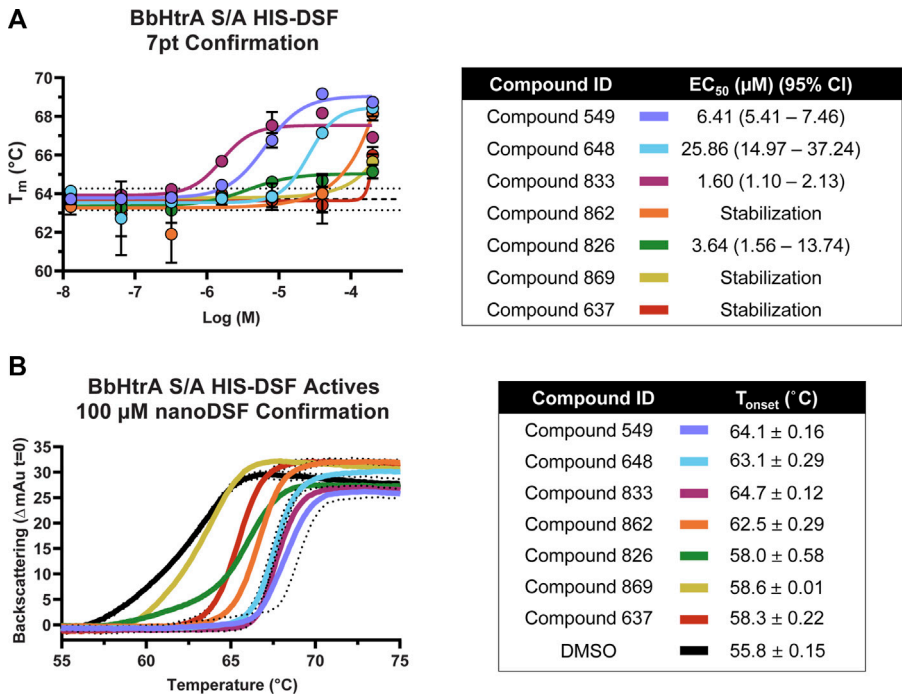

FIGURE 5
Confirmation and follow-up on the BbHtrA S/A hit molecules from the HIS-DSF primary screen. **(A)** Dose-response curves for the compounds that validated from the primary screen. Each point shown is the mean for five replicates at an individual concentration, with error bars representing the standard deviation of the replicates. The dose-response values were fit with a four-parameter log-logistic fit to derive the EC_{50} and 95% confidence interval. **(B)** Single dose stabilization as detected by nanoDSF for the 7 compounds that confirmed by dose-response HIS-DSF. The lines represent the mean backscattering signals for 3 replicates, with dotted lines representing the standard deviation of the mean.

0.44% CV) despite the higher percentage of DMSO (final DMSO 2%). Of the 16 compounds that were selected from primary screening, 8 compounds demonstrate either dose-response or top-dose stabilization of BbHtrA S/A, resulting in a 50% confirmation rate from the primary screening campaign (Figure 5A). Four of the confirmed compounds had full dose-response curves with upper and lower asymptotes, allowing for robust calculation of EC_{50} values using four-parameter log-logistic fits. Three hit molecules had HIS-DSF EC_{50} values below 10 μM (**549**: 6.41, **833**: 1.60, and **826**: 3.64 μM) (Figure 5A), while a fourth compound, **648** had an EC_{50} value of 25.86 μM. The remaining four confirmed compounds all had stabilization at the 200 μM concentration of drug that was above the filtering criteria ($T_{m(DMSO)} + 2\sigma_{Tm(DMSO)}$) but we were unable to derive an EC_{50} value.

Confirmation of thermal shift using nanoDSF and backscattering assays

In order to validate findings from the HIS-DSF assay, the 8 compounds that confirmed in 7-pt dose-response using HIS-DSF were tested using an orthogonal thermal shift-based method called nanoDSF, a differential scanning fluorimetry method that monitors shifts in tryptophan autofluorescence, as well as by monitoring backscattering aggregation signals during a thermal shift experiment (Kotov et al., 2019; Krakowiak et al., 2019; Magnusson et al., 2019; Baljinnyam et al., 2020a). Of the 8 compounds tested at 100 μM, 7 demonstrated a significant increase in the T_{onset}, or the temperature at which there is a significant onset of protein aggregation signal, as compared to the negative control (DMSO T_{onset} 55.8°C ± 0.15) (Figure 5B). This represents a confirmation rate of 87.5% from the validated HIS-DSF hits, and an overall hit rate of 0.8% for the entire primary screen. Importantly, there was a significant correlation (p: 0.0046, Pearson r: 0.8946) between the T_{onset} as determined by backscattering aggregation and the HIS-DSF T_m values (Supplementary Figure 1D).

Testing hit molecules for proteolytic inhibition

Hit molecules were further profiled for their ability to inhibit the protease activity of BbHtrA by monitoring the proteolytic digestion of a model substrate, casein. Compounds were tested in dose-response using a casein substrate that has been labeled with a molar excess of BODIPY dye, resulting in a quenched substrate that fluoresces only after proteolytic cleavage. Notably, hit molecules **549** and **833** demonstrate inhibition of BbHtrA

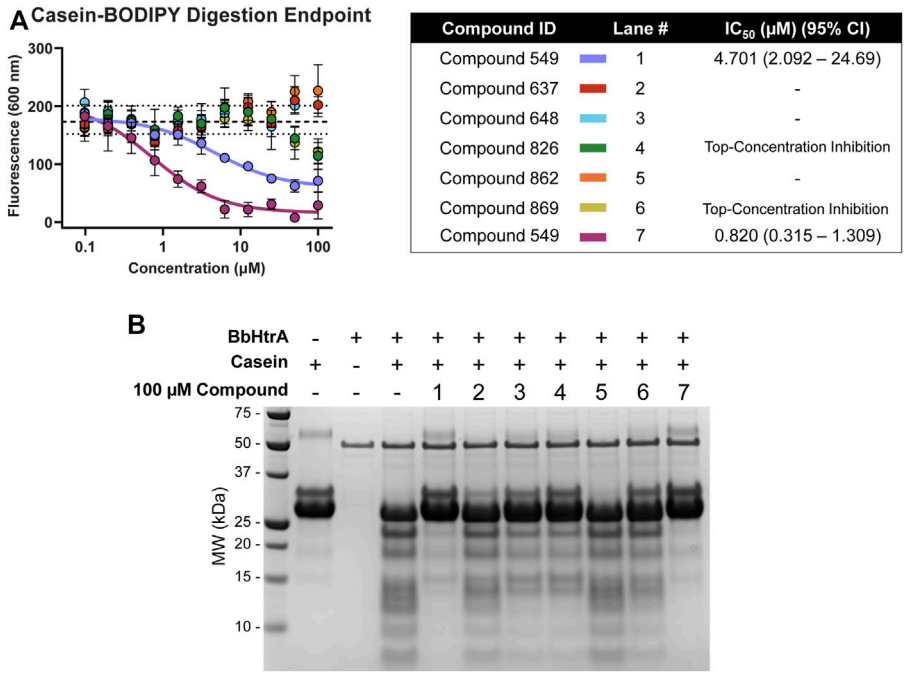

FIGURE 6
BbHtrA proteolytic activity in the presence of hit molecules. **(A)** Dose-response curves for hit molecules in a casein-BODIPY proteolysis assay using BbHtrA WT. Points represent the mean at each individual dose with error bars representing the standard deviation, with a dashed line and dotted lines representing the mean and ±2 standard deviations of negative control samples. The dose-response values are fit with a four-parameter log logistic fit to derive the IC_{50}. **(B)** SDS-PAGE gel of casein digests with BbHtrA WT in the presence of 100 μM compound. Gels were stained with Imperial Blue protein stain overnight.

proteolysis with an IC_{50} of 4.70 and 0.820 μM, respectively. Compounds **826** and **869** also demonstrate partial inhibition at higher concentrations, but we were unable to fit a log logistic curve to the data.

Further confirmation of proteolytic inhibition was given by testing native casein digestion in the presence of inhibitors and separation of digestion fragments by SDS-PAGE. The lack of casein cleavage products in compound lane 1 and 7 signifies near total inhibition of casein proteolysis with hit molecules **549** and **833** (Figure 6). **648**, **826**, and **869** all display partial inhibition of proteolysis, while molecules **637** and **862** don't appear to inhibit proteolytic activity of BbHtrA (Figure 6).

Discussion

Here, we have screened a library of 872 compounds that are known to target different classes of proteases for their ability to thermally stabilize BbHtrA. We applied a single-concentration approach to our primary screening and filtered hits by applying a selection criterion based on the standard deviation of the negative control that resulted in a hitlist of 16 compounds, a 1.6% hit rate in line with commonly reported HTS primary screens. The thermal-stabilizing effect of these hit compounds was confirmed in dose-response using the HIS-DSF assay, of which 50% were confirmed from the primary screen. These compounds were then confirmed independently of HIS-DSF using nanoDSF, in which 7 of the 8 compounds were shown to engage with BbHtrA. Additional characterization of these compounds in two independent caseinolytic assays shows that 5 of the 7 molecules can inhibit protease activity to varying degrees (Table 1).

By using a red-shifted fluorescent reporter that specifically binds to the protein of interest *via* polyhistidine affinity tag and is relatively insensitive to buffer composition, there is a considerable expansion to the applicability of the DSF assays that rely on extrinsic dyes to amplify the unfolding signal. While the use of a fluorophore in the red wavelengths cannot completely overcome interference from small molecule and buffer autofluorescence, it substantially reduces the number of false positive hits (Simeonov et al., 2008; Gao et al., 2020).

The interfering signal arising from detergent use with SYPRO Orange, resulting from dye that is shuttled into the hydrophobic milieu of the surfactant micelles, was not seen with the NTA fluorophore employed in this study. This is particularly important in a high-throughput setting where detergent use is practically necessary to prevent sticking to microfluidic lines and plateware. Additionally, the affinity-directed fluorophore will be considerably less sensitive to contaminating species present in

TABLE 1 Compilation of assay measurements for validated hits from the HIS-DSF screen.

Compound #	HIS-DSF potency (μM)	nanoDSF tonset (ΔDMSO °C)	Casein-BODIPY IC50 (μM)
549	6.41	8.3	4.701
637	Top Dose Stabilization	2.5	—
648	25.86	7.3	—
826	3.64	2.2	Top Dose Inhibition
833	1.6	8.9	0.82
862	Top Dose Stabilization	6.7	—
869	Top Dose Stabilization	2.8	Top Dose Inhibition

solution, potentially allowing for measurements in the presence of cofactors, binding partners, or even in a cellular lysate. While extrinsic molecular rotor and thiol-reactive dyes have been developed that can perform in the presence of surfactants, these fluorophores remain nonspecific and will detect any protein aggregation event (Ablinger et al., 2013; Bergsdorf and Wright, 2018; McClure et al., 2018).The DSF assay is sensitive to changes in the Gibbs free energy of the complex rather than any activity readout, and so compounds evolving from these biophysical campaigns are not necessarily bound to an active site of a target. Interestingly, compounds **637** and **862** were unable to inhibit protease activity against casein, despite having confirmed engagement with BbHtrA as shown by HIS-DSF and nanoDSF. This finding lends further power to the HIS-DSF assay in identifying binders that are potentially acting outside of the active site of a protein, presenting additional value for drug discovery projects and therapeutic targets that do not have any functional assay available or is not suitable for the screening campaign. The specificity of the HIS-tag system will also be of interest to fragment-screening campaigns that may require cofactors in solution that may interfere with nonspecific extrinsic dyes or screens that want to perform thermal shift analysis in complex solutions or lysates.

Data availability statement

The original contributions presented in the study are included in the article/Supplementary Material, further inquiries can be directed to the corresponding authors.

Author contributions

MR, BB, and AS designed the experiments and wrote the manuscript. MR and BB conducted experiments and analyzed and interpreted the data. MR and ZI worked to adapt instrumentation and create the workflows. MR, SJ, and AZ worked to create analysis scripts and methods to analyze raw data. UP and AS provided supervision and funding.

Funding

This research was supported by the Intramural Research Program of the NIH, National Center for Advancing Translational Sciences (NCATS) (ZIA TR000302-02 to AS).

Conflict of interest

The authors declare that the research was conducted in the absence of any commercial or financial relationships that could be construed as a potential conflict of interest.

Publisher's note

Supplementary material

The Supplementary Material for this article can be found online at: https://www.frontiersin.org/articles/10.3389/fphar.2022.1040039/full#supplementary-material

References

Ablinger, E., Leitgeb, S., and Zimmer, A. (2013). Differential scanning fluorescence approach using a fluorescent molecular rotor to detect thermostability of proteins in surfactant-containing formulations. *Int. J. Pharm.* 441, 255–260. doi:10.1016/j.ijpharm.2012.11.035

Amaning, K., Lowinski, M., Vallee, F., Steier, V., Marcireau, C., Ugolini, A., et al. (2013). The use of virtual screening and differential scanning fluorimetry for the rapid identification of fragments active against MEK1. *Bioorg. Med. Chem. Lett.* 23, 3620–3626. doi:10.1016/j.bmcl.2013.04.003

Backert, S., Bernegger, S., Skorko-Glonek, J., and Wessler, S. (2018). Extracellular HtrA serine proteases: An emerging new strategy in bacterial pathogenesis. *Cell. Microbiol.* 20, e12845. doi:10.1111/cmi.12845

Baljinnyam, B., Ronzetti, M., Yasgar, A., and Simeonov, A. (2020a2089). Applications of differential scanning fluorometry and related technologies in characterization of protein-ligand interactions. *Methods Mol. Biol.* 2089, 47–68. doi:10.1007/978-1-0716-0163-1_4

Baljinnyam, B., Ronzetti, M., Yasgar, A., and Simeonov, A. (2020b). "Applications of differential scanning fluorometry and related technologies in characterization of protein–ligand interactions," in *Targeting enzymes for pharmaceutical development: Methods and protocols*. Editor N. E. Labrou (New York, NY: Springer US).

Bergsdorf, C., and Wright, S. K. (2018). A guide to run affinity screens using differential scanning fluorimetry and surface plasmon resonance assays. *Methods Enzymol.* 610, 135–165. doi:10.1016/bs.mie.2018.09.015

Bernard, Q., Thakur, M., Smith, A. A., Kitsou, C., Yang, X., and Pal, U. (2019). Borrelia burgdorferi protein interactions critical for microbial persistence in mammals. *Cell. Microbiol.* 21, e12885. doi:10.1111/cmi.12885

Bernegger, S., Brunner, C., Vizovisek, M., Fonovic, M., Cuciniello, G., Giordano, F., et al. (2020). A novel FRET peptide assay reveals efficient *Helicobacter pylori* HtrA inhibition through zinc and copper binding. *Sci. Rep.* 10, 10563. doi:10.1038/s41598-020-67578-2

Biter, A. B., De La Pena, A. H., Thapar, R., Lin, J. Z., and Phillips, K. J. (2016). DSF guided refolding as A novel method of protein production. *Sci. Rep.* 6, 18906. doi:10.1038/srep18906

Cho, H., Choi, Y., Min, K., Son, J. B., Park, H., Lee, H. H., et al. (2020). Over-activation of a nonessential bacterial protease DegP as an antibiotic strategy. *Commun. Biol.* 3, 547. doi:10.1038/s42003-020-01266-9

Christine, C. G., and Wright, S. K. (2017). Biophysics: For HTS hit validation, chemical lead optimization, and beyond. *Expert Opin. Drug Discov.* 12, 897–907. doi:10.1080/17460441.2017.1349096

Clausen, T., Kaiser, M., Huber, R., and Ehrmann, M. (2011). HTRA proteases: Regulated proteolysis in protein quality control. *Nat. Rev. Mol. Cell. Biol.* 12, 152–162. doi:10.1038/nrm3065

Clausen, T., Southan, C., and Ehrmann, M. (2002). The HtrA family of proteases: Implications for protein composition and cell fate. *Mol. Cell.* 10, 443–455. doi:10.1016/s1097-2765(02)00658-5

Desantis, K. A., and Reinking, J. L. (2016). Use of differential scanning fluorimetry to identify nuclear receptor ligands. *Methods Mol. Biol.* 1443, 21–30. doi:10.1007/978-1-4939-3724-0_3

Gao, K., Oerlemans, R., and Groves, M. R. (2020). Theory and applications of differential scanning fluorimetry in early-stage drug discovery. *Biophys. Rev.* 12, 85–104. doi:10.1007/s12551-020-00619-2

Gherardini, F. C. (2013). Borrelia burgdorferi HtrA may promote dissemination and irritation. *Mol. Microbiol.* 90, 209–213. doi:10.1111/mmi.12390

Ibrahim, Y. M., Kerr, A. R., Mccluskey, J., and Mitchell, T. J. (2004). Role of HtrA in the virulence and competence of Streptococcus pneumoniae. *Infect. Immun.* 72, 3584–3591. doi:10.1128/IAI.72.6.3584-3591.2004

Jarmoskaite, I., Alsadhan, I., Vaidyanathan, P. P., and Herschlag, D. (2020). How to measure and evaluate binding affinities. *eLife* 9, e57264. doi:10.7554/eLife.57264

Jerabek-Willemsen, M., Wienken, C. J., Braun, D., Baaske, P., and Duhr, S. (2011). Molecular interaction studies using microscale thermophoresis. *Assay. Drug Dev. Technol.* 9, 342–353. doi:10.1089/adt.2011.0380

Kariu, T., Sharma, K., Singh, P., Smith, A. A., Backstedt, B., Buyuktanir, O., et al. (2015). BB0323 and novel virulence determinant BB0238: Borrelia burgdorferi proteins that interact with and stabilize each other and are critical for infectivity. *J. Infect. Dis.* 211, 462–471. doi:10.1093/infdis/jiu460

Kariu, T., Yang, X., Marks, C. B., Zhang, X., and Pal, U. (2013). Proteolysis of BB0323 results in two polypeptides that impact physiologic and infectious phenotypes in Borrelia burgdorferi. *Mol. Microbiol.* 88, 510–522. doi:10.1111/mmi.12202

Kotov, V., Bartels, K., Veith, K., Josts, I., Subhramanyam, U. K. T., Günther, C., et al. (2019). High-throughput stability screening for detergent-solubilized membrane proteins. *Sci. Rep.* 9, 10379. doi:10.1038/s41598-019-46686-8

Krakowiak, J., Krajewska, M., and Wawer, J. (2019). Monitoring of lysozyme thermal denaturation by volumetric measurements and nanoDSF technique in the presence of N-butylurea. *J. Biol. Phys.* 45, 161–172. doi:10.1007/s10867-019-09521-9

Krasavin, M., Kalinin, S., Zozulya, S., Gryniukova, A., Borysko, P., Angeli, A., et al. (2020). Screening of benzenesulfonamide in combination with chemically diverse fragments against carbonic anhydrase by differential scanning fluorimetry. *J. Enzyme Inhib. Med. Chem.* 35, 306–310. doi:10.1080/14756366.2019.1698562

Krojer, T., Garrido-Franco, M., Huber, R., Ehrmann, M., and Clausen, T. (2002). Crystal structure of DegP (HtrA) reveals a new protease-chaperone machine. *Nature* 416, 455–459. doi:10.1038/416455a

Lee, M. E., Dou, X., Zhu, Y., and Phillips, K. J. (2019). Refolding proteins from inclusion bodies using differential scanning fluorimetry guided (DGR) protein refolding and MeltTraceur web. *Curr. Protoc. Mol. Biol.* 125, e78. doi:10.1002/cpmb.78

Li, X., and Zhang, C. (2021). Using differential scanning fluorimetry (DSF) to detect ligand binding with purified protein. *Methods Mol. Biol.* 2213, 183–186. doi:10.1007/978-1-0716-0954-5_16

Magnusson, A. O., Szekrenyi, A., Joosten, H. J., Finnigan, J., Charnock, S., and Fessner, W. D. (2019). nanoDSF as screening tool for enzyme libraries and biotechnology development. *FEBS J.* 286, 184–204. doi:10.1111/febs.14696

Mcclure, S. M., Ahl, P. L., and Blue, J. T. (2018). High throughput differential scanning fluorimetry (DSF) formulation screening with complementary dyes to assess protein unfolding and aggregation in presence of surfactants. *Pharm. Res.* 35, 81. doi:10.1007/s11095-018-2361-1

Nie, M., Liu, Y., Huang, X., Zhang, Z., and Zhao, Q. (2022). Microtiter plate-based differential scanning fluorimetry: A high-throughput method for efficient formulation development. *J. Pharm. Sci.* 111, 2397–2403. doi:10.1016/j.xphs.2022.05.015

Niesen, F. H., Berglund, H., and Vedadi, M. (2007). The use of differential scanning fluorimetry to detect ligand interactions that promote protein stability. *Nat. Protoc.* 2, 2212–2221. doi:10.1038/nprot.2007.321

Pallen, M. J., and Wren, B. W. (1997). The HtrA family of serine proteases. *Mol. Microbiol.* 26, 209–221. doi:10.1046/j.1365-2958.1997.5601928.x

Pantoliano, M. W., Petrella, E. C., Kwasnoski, J. D., Lobanov, V. S., Myslik, J., Graf, E., et al. (2001). High-density miniaturized thermal shift assays as a general strategy for drug discovery. *J. Biomol. Screen.* 6, 429–440. doi:10.1177/108705710100600609

Ronzetti, M., Baljinnyam, B., Jalal, I., Pal, U., and Simeonov, A. (2022). Application of biophysical methods for improved protein production and characterization: A case study on an HtrA-family bacterial protease. *Protein Sci.*, e4498. doi:10.1002/pro.4498

Russell, T. M., Delorey, M. J., and Johnson, B. J. (2013). Borrelia burgdorferi BbHtrA degrades host ECM proteins and stimulates release of inflammatory cytokines *in vitro*. *Mol. Microbiol.* 90, 241–251. doi:10.1111/mmi.12377

Russell, T. M., Tang, X., Goldstein, J. M., Bagarozzi, D., and Johnson, B. J. (2016). The salt-sensitive structure and zinc inhibition of Borrelia burgdorferi protease BbHtrA. *Mol. Microbiol.* 99, 586–596. doi:10.1111/mmi.13251

Seo, D. H., Jung, J. H., Kim, H. Y., and Park, C. S. (2014). Direct and simple detection of recombinant proteins from cell lysates using differential scanning fluorimetry. *Anal. Biochem.* 444, 75–80. doi:10.1016/j.ab.2013.09.027

Shao, H., Oltion, K., Wu, T., and Gestwicki, J. E. (2020). Differential scanning fluorimetry (DSF) screen to identify inhibitors of Hsp60 protein-protein interactions. *Org. Biomol. Chem.* 18, 4157–4163. doi:10.1039/d0ob00928h

Simeonov, A., Jadhav, A., Thomas, C. J., Wang, Y., Huang, R., Southall, N. T., et al. (2008). Fluorescence spectroscopic profiling of compound libraries. *J. Med. Chem.* 51, 2363–2371. doi:10.1021/jm701301m

SimeonoV, A. (2013). Recent developments in the use of differential scanning fluorometry in protein and small molecule discovery and characterization. *Expert Opin. Drug Discov.* 8, 1071–1082. doi:10.1517/17460441.2013.806479

Stricker, R. B., and Johnson, L. (2013). Borrelia burgdorferi aggrecanase activity: More evidence for persistent infection in Lyme disease. *Front. Cell. Infect. Microbiol.* 3, 40. doi:10.3389/fcimb.2013.00040

Thakur, M., Bista, S., Foor, S. D., Dutta, S., Yang, X., Ronzetti, M., et al. (2022). Controlled proteolysis of an essential virulence determinant dictates infectivity of Lyme disease pathogens. *Infect. Immun.* 90, e0005922. doi:10.1128/iai.00059-22

Wang, Y., Van Oosterwijk, N., Ali, A. M., Adawy, A., Anindya, A. L., Domling, A. S. S., et al. (2017). A systematic protein refolding screen method using the DGR approach reveals that time and secondary TSA are essential variables. *Sci. Rep.* 7, 9355. doi:10.1038/s41598-017-09687-z

Ye, M., Sharma, K., Thakur, M., Smith, A. A., Buyuktanir, O., Xiang, X., et al. (2016). HtrA, a temperature- and stationary phase-activated protease involved in maturation of a key microbial virulence determinant, facilitates Borrelia burgdorferi infection in mammalian hosts. *Infect. Immun.* 84, 2372–2381. doi:10.1128/IAI.00360-16

Zhuang, X., Yang, X., Altieri, A. S., Nelson, D. C., and Pal, U. (2018). Borrelia burgdorferi surface-located Lmp1 protein processed into region-specific polypeptides that are critical for microbial persistence. *Cell. Microbiol.* 20, e12855. doi:10.1111/cmi.12855

Zurawa-Janicka, D., Skorko-Glonek, J., and Lipinska, B. (2010). HtrA proteins as targets in therapy of cancer and other diseases. *Expert Opin. Ther. Targets* 14, 665–679. doi:10.1517/14728222.2010.487867